**Supporting Information**

# *In situ* Disorder-Order Transformation in Synthetic Gallosilicate Zeolites with the NAT Topology

Suk Bong Hong,[*,†] Song-Ho Lee,[†] Chae-Ho Shin,[‡] Ae Ja Woo,[§] Luis J. Alvarez,[□] Claudio M. Zicovich-Wilson,[⊥] and Miguel A. Camblor[#]

[†]*Division of Chemical Engineering, Hanbat National University, Taejon 305-719, Korea,* [‡]*Department of Chemical Engineering, Chungbuk National University, Chungbuk 361-763, Korea,* [§]*Department of Science Education, Ewha Womans University, Seoul 120-750, Korea,* [□]*Instituto de Matématicas (U. Cuernavaca), Universidad Nacional Autónoma de Mexico, 62210 Cuernavaca (Mor), Mexico,* [⊥]*Facultad de Ciencias, Universidad Autónoma del Estado de Morelos, 62210 Cuernavaca (Mor), Mexico, and* [#]*Instituto de Ciencia de Materiales de Madrid, Consejo Superior de Investigaciones Científicas Campus Cantoblanco, 28049 Madrid, Spain*

***Table 1S*. Fractional Atomic Coordinates of the Asymmetric Units of the Four Optimized Periodic Models Considered for *Ab Initio* Calculations ($\omega_1$, $\tau_1$, $\tau_2$, $\tau_3$; See Table 1 and Text). In All Cases, the Primitive Cell Choice, with Parameters: *a* = *b* = *c* = 9.90788 Å, α = β = 96.4919°, and γ = 140.7032°, Has Been Considered.**

Model $\omega_1$

| atom | *x* | *y* | *z* |
|---|---|---|---|
| Si | -0.0607 | 0.0112 | 0.1981 |
| Ga | -0.1842 | -0.4955 | -0.4342 |
| Si | -0.4885 | -0.4885 | 0.0000 |
| O | 0.1663 | 0.1027 | 0.2022 |
| O | -0.4380 | 0.2621 | 0.4077 |
| O | 0.3626 | -0.0152 | 0.1307 |
| O | -0.2819 | -0.2644 | 0.1442 |
| O | 0.0672 | -0.2860 | -0.4830 |
| Na | 0.3605 | 0.2879 | 0.4404 |

Model $\tau_1$

| atom | *x* | *y* | *z* |
|---|---|---|---|
| Si | -0.0627 | 0.0101 | 0.1892 |
| Ga | -0.2046 | 0.4973 | -0.4386 |
| Si | -0.5000 | -0.5000 | 0.0000 |
| Si | 0.2500 | -0.2500 | -0.5000 |
| O | 0.1032 | 0.0088 | 0.1764 |
| O | -0.4666 | 0.2450 | 0.4209 |
| O | 0.3536 | -0.0035 | 0.1121 |
| O | -0.3267 | -0.2548 | 0.1216 |
| O | 0.0453 | -0.3012 | 0.4975 |
| Na | 0.1799 | 0.0008 | 0.4235 |

Model $\tau_2$

| atom | *x* | *y* | *z* |
|---|---|---|---|
| Ga | -0.0812 | 0.0099 | 0.1766 |
| Si | -0.1655 | -0.2605 | -0.1737 |
| Si | -0.2434 | 0.1690 | -0.3261 |
| Si | 0.4995 | 0.0829 | 0.3107 |
| Si | 0.4931 | 0.4874 | -0.0026 |
| O | 0.0983 | 0.0063 | 0.1760 |
| O | -0.1644 | -0.0932 | -0.1561 |
| O | -0.2673 | 0.3151 | -0.3011 |
| O | -0.3412 | 0.0733 | 0.2991 |
| O | 0.3750 | 0.0216 | 0.1466 |
| O | -0.1250 | 0.2010 | -0.1740 |
| O | -0.2233 | -0.3668 | -0.3380 |
| O | -0.3816 | -0.2852 | 0.1104 |
| O | -0.3622 | -0.4636 | -0.1080 |
| O | -0.4960 | -0.0997 | -0.4035 |
| O | 0.3044 | -0.1225 | 0.3735 |
| Na | 0.3460 | -0.3923 | 0.2194 |

Model $\tau_3$

| atom | *x* | *y* | *z* |
|---|---|---|---|
| Si | -0.0880 | 0.0004 | 0.1779 |
| Si | -0.1554 | -0.4782 | -0.4148 |
| Si | -0.2209 | 0.2023 | -0.3188 |
| Si | 0.2356 | 0.0534 | 0.0781 |
| Ga | 0.4852 | 0.4852 | 0.0000 |
| Ga | 0.2715 | -0.2285 | -0.5000 |
| O | 0.1411 | 0.0952 | 0.1778 |
| O | -0.3901 | 0.2880 | 0.4549 |
| O | -0.1026 | 0.4473 | -0.2997 |
| O | 0.0124 | -0.1896 | -0.0503 |
| O | 0.3772 | 0.0503 | 0.1742 |
| O | -0.2034 | -0.3718 | -0.3329 |
| O | -0.3088 | -0.2654 | 0.1581 |
| O | 0.0564 | -0.2850 | -0.4678 |
| O | -0.4873 | 0.0176 | -0.3422 |
| O | 0.4012 | 0.2433 | 0.0007 |
| Na | 0.4213 | 0.1567 | -0.2275 |

***Table 2S*. Experimental $^{29}$Si NMR Chemical Shifts of a Completely Ordered Aluminosilicate Natrolite in the Orthorhombic Symmetry vs the Isotopic Chemical Shifts Predicted from the Average T-O-T Angles Taken in the Crystallographic Data for Two Materials with the Same Space group (*Fdd*2) and Si/Al ratio (Si/Al = 1.50)**

| Si site | multiplicity | average ∠T-O-T[a] | structural unit | $^{29}$Si δ (ppm) | | | | | average ∠T-O-T[h] | structural unit | $^{29}$Si δ (ppm) | | | | |
|---|---|---|---|---|---|---|---|---|---|---|---|---|---|---|---|
| | | | | $\delta_{pre1}$[b,c] | $\delta_{pre2}$[c,d] | $\delta_{obs}$[e] | $\Delta\delta_1$[f] | $\Delta\delta_2$[g] | | | $\delta_{pre1}$[b,c] | $\delta_{pre2}$[c,d] | $\delta_{obs}$[e] | $\Delta\delta_1$[f] | $\Delta\delta_2$[g] |
| $Si_2$ | 8 | 142.5 | $Si_2$(4Al) | -85.4 | -86.3 | | | | 142.4 | $Si_2$(4Al) | -85.3 | -86.2 | | | |
| | | | $Si_2$(3Al) | -91.0 | -91.3 | | | | | $Si_2$(3Al) | -90.9 | -91.2 | | | |
| | | | $Si_2$(2Al) | -96.6 | -96.3 | -95.2 | 1.4 | 1.1 | | $Si_2$(2Al) | -96.5 | -96.2 | -95.2 | 1.3 | 1.0 |
| | | | $Si_2$(1Al) | -102.2 | -101.3 | | | | | $Si_2$(1Al) | -102.1 | -101.2 | | | |
| | | | $Si_2$(0Al) | -107.8 | -106.3 | | | | | $Si_2$(0Al) | -107.7 | -106.2 | | | |
| $Si_1$ | 16 | 136.8 | $Si_1$(4Al) | -81.1 | -81.6 | | | | 137.0 | $Si_1$(4Al) | -81.3 | -81.8 | | | |
| | | | $Si_1$(3Al) | -86.7 | -86.6 | -87.6 | -1.1 | -1.0 | | $Si_1$(3Al) | -86.9 | -86.8 | -87.6 | -0.7 | -0.8 |
| | | | $Si_1$(2Al) | -92.3 | -91.6 | | | | | $Si_1$(2Al) | -92.5 | -91.8 | | | |
| | | | $Si_1$(1Al) | -97.9 | -96.6 | | | | | $Si_1$(1Al) | -98.1 | -96.8 | | | |
| | | | $Si_1$(0Al) | -103.5 | -101.6 | | | | | $Si_1$(0Al) | -103.7 | -101.8 | | | |

[a]Average T-O-T angles in degrees from the crystallographic data reported by Artioli et al. (*Acta Cryst.* **1984**, *C40*, 1658). [b]Predicted chemical shifts from the average T-O-T angles using the equation of Ramdas and Klinowskii (*Nature* **1984**, *308*, 521). [c]The $T'_1$ sites with a multiplicity of 16 are assumed to be exclusively occupied by Al atoms. [d]Predicted chemical shifts from the average T-O-T angles using the equation of Radeglia and Engelhardt (*Chem. Phys. Lett.* **1985**, *114*, 28). [e]Experimental chemical shifts reported by Neuhoff et al. (*Am. Mineral.* **2002**, *87*, 1307). [f]$\Delta\delta_1 = \delta_{obs} - \delta_{pre1}$. [g]$\Delta\delta_2 = \delta_{obs} - \delta_{pre2}$. [h]Average T-O-T angles in degrees from the crystallographic data reported by Meneghinello et al. (*Microporous Mesoporous Mater.* **1999**, *30*, 89).

***Table 3S*. Chemical Shifts and Relative Intensities of the $^{29}$Si MAS NMR Resonances from the Six Gallosilicate NAT Materials Prepared at 150 °C for 3-23 days and Their Si/Ga Ratios Calculated by $^{29}$Si MAS NMR**

| line ID[a] | NAT-150-3 | | NAT-150-5 | | NAT-150-7 | | NAT-150-10 | | NAT-150-14 | | NAT-150-23 | |
|---|---|---|---|---|---|---|---|---|---|---|---|---|
| | δ, ppm | *I*, % | δ, ppm | *I*, % | δ, ppm | *I*, % | δ, ppm | *I*, % | δ, ppm | *I*, % | δ, ppm | *I*, % |
| A | -74.3 | 1.6 | -74.5 | 1.6 | -74.3 | 1.5 | -74.3 | 0.7 | -74.3 | 0.7 | -74.3 | 1.1 |
| B | -79.1 | 10.7 | -78.9 | 8.7 | -78.0 | 9.5 | -78.7 | 5.7 | -78.6 | 2.8 | -78.6 | 1.9 |
| C | -82.0 | 4.4 | -81.9 | 3.7 | -81.7 | 7.8 | -82.0 | 5.0 | -82.0 | 4.2 | -82.0 | 5.2 |
| D | -84.7 | 30.0 | -84.6 | 37.0 | -83.7 | 35.4 | -84.3 | 42.6 | -84.3 | 55.5 | -84.3 | 53.5 |
| E | -88.3 | 15.3 | -88.1 | 11.7 | -87.4 | 12.1 | -87.6 | 11.3 | -87.0 | 5.8 | -87.0 | 6.7 |
| F | -91.0 | 11.0 | -91.0 | 7.4 | -91.0 | 7.4 | -91.0 | 7.2 | -91.0 | 4.2 | -91.0 | 4.8 |
| G | -94.2 | 14.9 | -94.4 | 17.0 | -93.7 | 16.8 | -94.1 | 20.1 | -94.1 | 23.0 | -94.1 | 23.6 |
| H | -98.4 | 8.5 | -98.4 | 7.6 | -98.0 | 7.5 | -98.0 | 5.6 | -97.5 | 2.8 | -97.5 | 1.9 |
| I | -101.5 | 3.6 | -101.5 | 5.3 | -101.5 | 2.0 | -101.3 | 1.8 | -101.3 | 1.0 | -101.3 | 1.3 |
| $Si/Ga_{nmr,I\text{-}42d}$[b] | 1.75 | | 1.78 | | 1.69 | | - | | - | | - | |
| $Si/Ga_{nmr,Fdd2}$[c] | 1.51 (1.55) | | 1.53 (1.58) | | 1.46 (1.59) | | 1.49 (1.55) | | 1.47 (1.57) | | 1.47 (1.57) | |
| $I_D/I_G$[d] | 2.01 | | 2.18 | | 2.19 | | 2.12 | | 2.41 | | 2.27 | |
| $Si/Ga_{nmr,D+G}$[e] | 1.50 | | 1.49 | | 1.49 | | 1.49 | | 1.48 | | 1.49 | |

[a]Line ID's are the same as those given in Figure 7 or Table 3. [b]The Si/Ga ratio calculated from the tetragonal assignments of their $^{29}$Si MAS NMR NMR data. The values for NAT-150-10, NAT-150-14, and NAT-150-23 were not calculated here, since the XRD patterns of these three materials were not indexable as tetragonal. [c]The Si/Ga ratio calculated according to the orthorhombic assignments of their NMR data. The values in parentheses are the Si/Ga ratio determined by elemental analysis. [d]The relative intensity ratio of line D to Line G that are assigned to $Si_1(3Ga)$ and $Si_2(2Ga)$ species in the orthorhombic model, respectively. [e]The Si/Ga ratio calculated using lines D and G only based on the orthorhombic assumption.

***Table 4S.*** **Fractional Occupation of Ga in the Different Nonequivalent T-sites for the Ordered and Disordered Simulated Structures**

| Si/Ga | *ordered* | *disordered* | | | |
|---|---|---|---|---|---|
| | 1.50 | 1.50 | 1.53 | 1.55 | 1.58 |
| $T_1$ | 0.00 | 0.44 | 0.43 | 0.43 | 0.43 |
| $T'_1$ | 1.00 | 0.44 | 0.44 | 0.43 | 0.43 |
| $T_2$ | 0.00 | 0.25 | 0.24 | 0.23 | 0.21 |

***Table 5S*. Percentages of 4-Rings Composed only of $T_1$ Sites with *n*Ga Atoms for the Ordered and Disordered Simulated Structures[a]**

| *n* // Si/Ga | *ordered* | *disordered* | | | |
|---|---|---|---|---|---|
| | 1.50 | 1.50 | 1.53 | 1.55 | 1.58 |
| 0 | 0.0 | 1.94 | 1.95 | 1.94 | 1.92 |
| 1 | 0.0 | 21.53 | 22.46 | 23.13 | 23.90 |
| 2 | 100.0 | 76.29 | 75.34 | 74.67 | 73.90 |

[a] The very low percentage (< 0.3%) for the presence of 3 Ga atoms per 4-ring in each disordered structure, yielding violations of Loewenstein's rule, is not included.

**Figure 1S**. (a) $^{71}$Ga and (b) $^{23}$Na MAS NMR spectra of the NAT-150-3 (bottom) and NAT-150-23 (top) materials recorded at 150 ºC. Spinning side bands are marked by asterisks.

**Figure 2S**. $^{29}$Si MAS NMR spectra of (a) NAT-150-3, (b) NAT-150-5, (c) NAT-150-7, (d) NAT-150-10, (e) NAT-150-14, and (f) NAT-150-23 materials: experimental (top); simulated (middle); deconvoluted components (bottom). The best-simulated spectrum was obtained when the experimental one for each gallosilicate material is deconcoluted into 9 components denoted (from left to right) as lines A-I.

**Figure 3S**. Si(*n*Ga) populations as a function of the orthorhombic distortion. The populations calculated for the "disordered" model derived by *Monte Carlo* sampling (Si/Ga = 1.58) are shown at $\delta_o$ = 0.000, while those corresponding to the ordered model are arbitrarily depicted at $\delta_o$ = 0.029. The rest of values correspond to the experimental ones obtained from the orthorhombic assignment of the $^{29}$Si MAS NMR data. The square, diamond, and circle denote $T_1$, $T_2$, and total T ($T_1$ + $T_2$) populations, respectively.

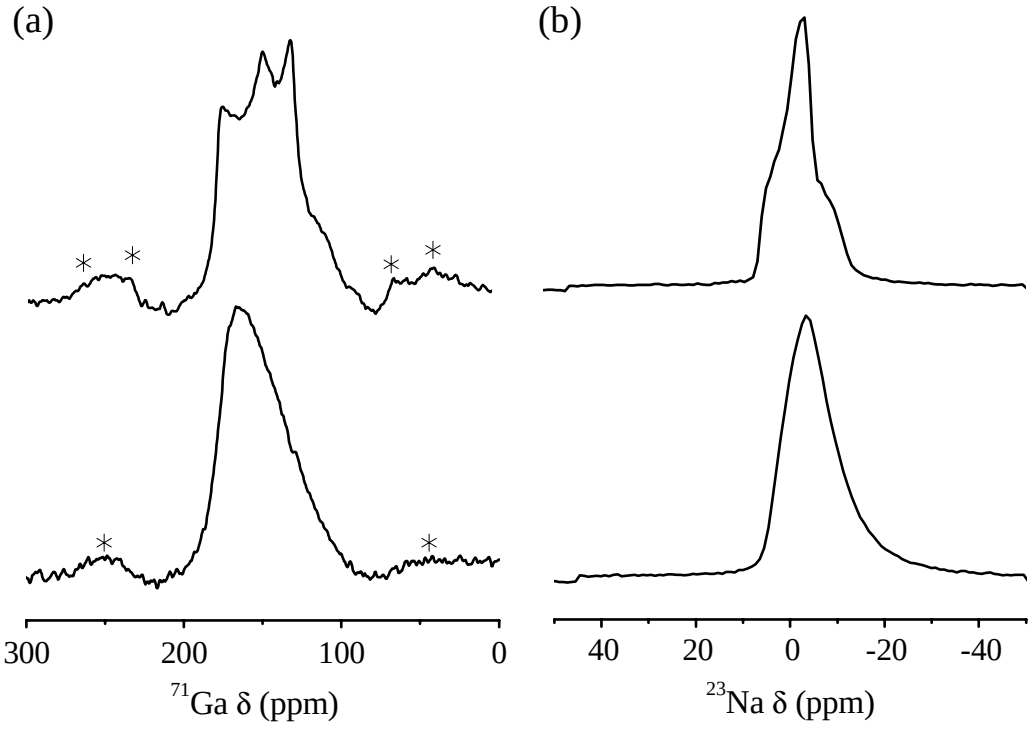


Figure 1S

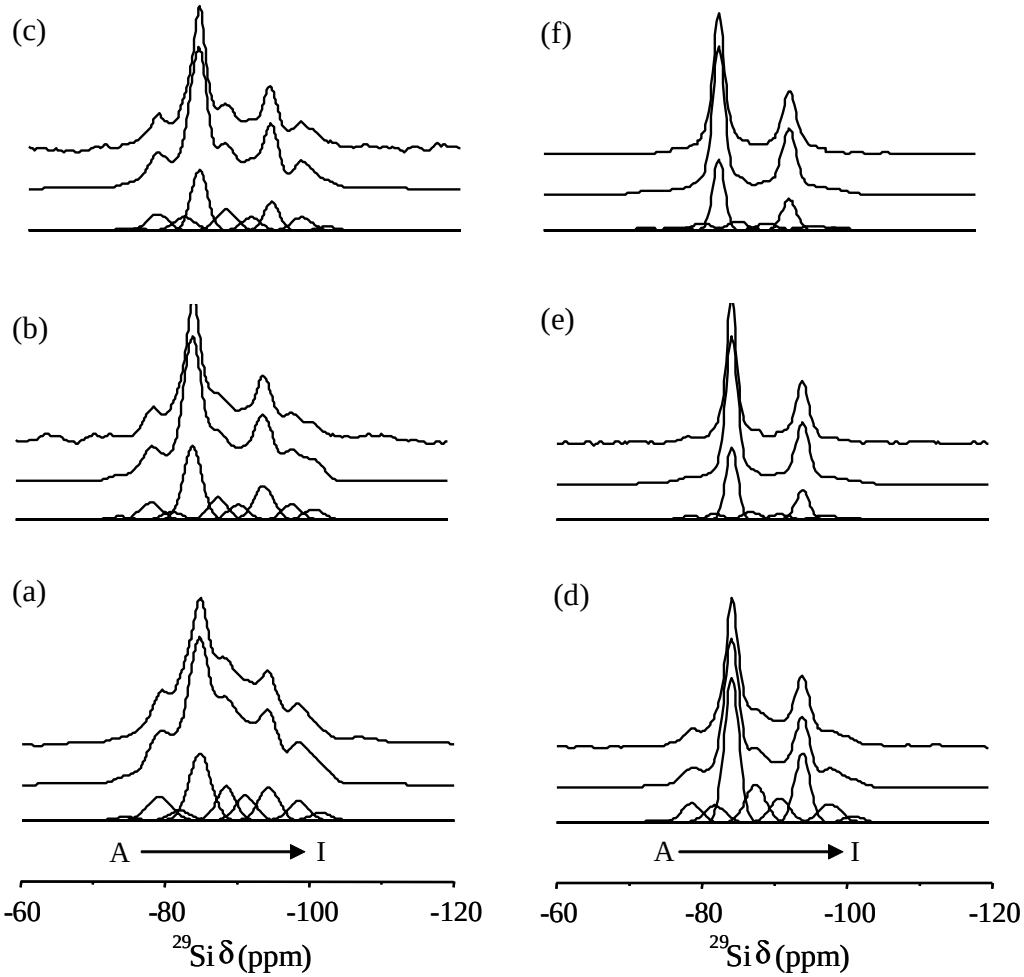


Figure 2S

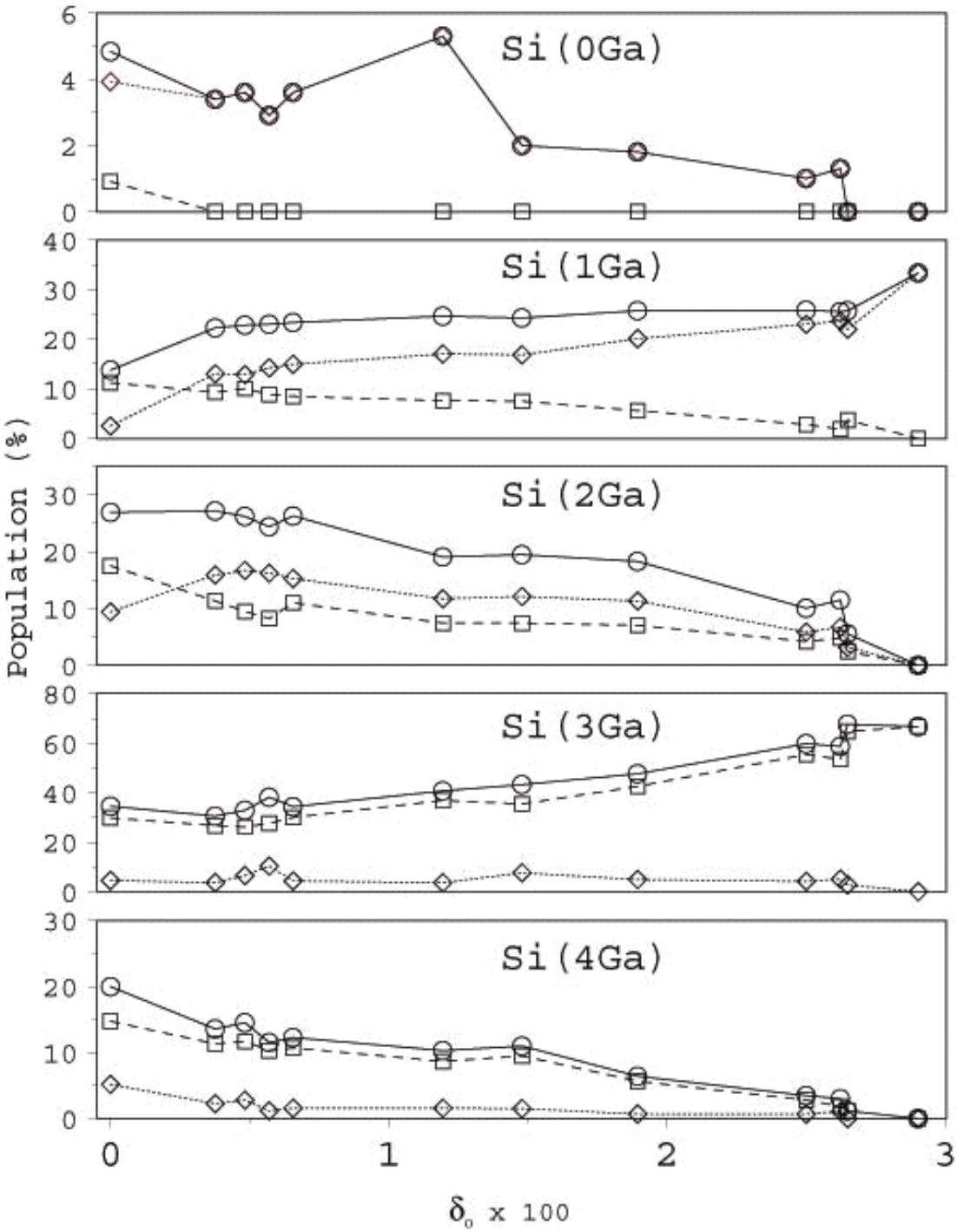


Figure 3S